Hydroentanglement Nonwoven Filters for Air Filtration and Its Performance Evaluation

Asis Patanaik,[1] Rajesh D. Anandjiwala[1,2]

[1]*CSIR Materials Science and Manufacturing, Fibres and Textiles Competence Area, Port Elizabeth 6000, South Africa*
[2]*Department of Textile Science, Faculty of Science, Nelson Mandela Metropolitan University, Port Elizabeth 6031, South Africa*

Received 13 February 2009; accepted 5 April 2009
DOI 10.1002/app.30561
Published online 29 March 2010 in Wiley InterScience (www.interscience.wiley.com).

ABSTRACT: New nonwoven filters are developed for air filtration application with the help of hydroentanglement bonding technique. Different types of nonwoven filters are produced by varying the hydroentanglement processing parameters. The changes in nonwoven filter properties after prolonged exposure to working conditions under cyclic compression play an important role in its long-term performance characteristics. The performance of the developed filters are evaluated in terms of changes in pore characteristics, filtration parameters, and strength after cyclic compression and compared with the corresponding values before subjecting it to cyclic compression. The developed filter shows good performance characteristics for air filtration with low pressure drop and high efficiency in capturing micron and submicron size particles without any significant changes in its strength. Theoretical understanding of the fluid flow emerging from the nozzles during the hydroentanglement process is simulated by the computational fluid dynamics (CFD). Based on the fluid drag force and impact force of the water jets, a mechanism of fiber bonding is proposed. The impact force of the water jets and fluid drag forces plays an important role in the mechanism of fiber bonding. Nozzle condition also plays an important role in economizing this process.
 J Appl Polym Sci 117: 1325–1331, 2010

Key words: compression; fibers; orientation; simulations

INTRODUCTION

Fiber-based filter is one of the fastest growing segments in the high-performance applications of flexible materials. The filter media uses a permeable material for the separation of particles passing through it. Nonwoven filters are essential part of industrial processes, contributing to product purity, savings in energy, production cost and cleaner environment. Nonwovens are characterized by the presence of micron and submicron size pores in its structures, making them preferred medium for air and liquid filtration applications.[1] When nonwoven filters are used for long period of time during air filtrations, they are subjected to cyclic compression at various stages due to cyclic variation in pressure.[2] The probable reason for this cyclic compression is due to the deposition of layers of dust particles on the filters resulting in the obstruction of the airflow. This causes the build up of pressure and cyclic variation in pressure, and it may affect the long-term performance characteristics of filters. For the development of high-efficiency filters for air filtration application, it is always necessary to have filters that can be used for longer period without any significant changes in filtration parameters, pore characteristics, and strength values.

The process of bonding the fiber web with the help of high-pressure water jets is known as hydroentanglement bonding technique. It is one of the popular mechanical methods of manufacturing nonwovens as the resulting material is strong and flexible.[3–5] A series of high-pressure columnar water jets is produced by pumping water through the micron sized conical capillary nozzles placed in a jet strip. These strips are clamped into different manifolds or pressure heads. High-velocity water jets emerging from the nozzles are directed to the incoming fibrous web supported on a moving conveyer. These water jets exert enough force on the fibers to entangle them with each other, resulting in the formation of nonwoven fabric, and most of the deenergized water is drawn through the conveyer by suction for recycling and reuse. Generally multiple manifolds with different water jet pressure are used to produce a well bonded fabric.[6]

Despite some published work on the aspect of bonding the fibrous web with the help of high-pressure water jets,[5–7] the exact mechanism of bonding in terms of the fluid interaction with fibers is not yet

Correspondence to: A. Patanaik (patnaik_asis@yahoo.com).

well understood. The influence of the fluid drag forces acting on the fibers as a result of the impact force of the water jets is also not known. These forces play a key role in bonding the fibers, which result in the formation of nonwoven fabrics. So, an attempt has been made in this study to understand the mechanics of fiber bonding.

The hydroentanglement process is an energy intensive process, and how best the impact energy of the water jets is used properly plays an important role in determining the economics of the process. The conical capillary nozzles are the main component of this process; it is worthwhile to study the condition of these nozzles and fluid flow through them during the hydroentanglement process. The energy transformation depends on the applied water jet pressure and impact force of water jets, nature of the perforated surface (conveyer), and other factors. Fluid flow and related phenomena can be described by computational fluid dynamics (CFD). Because reported studies in CFD are very few,[8–10] new CFD simulation needs to be developed for the better understanding of the fluid flow through the nozzles during this process. CFD modeling was accomplished by the software Comsol Multiphysics.[11]

The performance of the developed filters are evaluated in terms of changes in pore characteristics, filtration parameters, and strength after cyclic compression and compared with the corresponding values before cyclic compression. Various types of pore sizes are measured by capillary flow porometer.[12] The fiber orientation in the nonwoven fabrics are measured by image analysis programme "analySIS" version 3.2.[13] For the measurement of filtration parameters, such as filtration efficiency and pressure drop, ASHRAE standard 52.2 was adopted,[14] and the dust filtration device was used. The tensile strength of the nonwoven fabrics was measured according to ISO standard 9073-3.[15]

EXPERIMENTAL

Sample preparation

Polyester fibers are used for nonwoven sample preparation. First, a carded web of the fibers is prepared, and then the web is oriented in the cross machine direction by using a crosslapper. This web is transported to the hydroentanglement unit containing three manifolds by a conveyor. Subsequently, fiber web is subjected to the action of high-pressure water jets emerging from the above manifolds. These manifolds are named as Manifolds 1, 2, and 3, respectively. Two different pressure ranges (60 and 120 bar) are selected in the manifolds for sample preparation. for Sample S1, the jet pressures kept in bar were 10, 60, 60, and for Sample S2 these values were 10, 120, 120, in the Manifolds 1, 2, and 3, respectively. Acrylate chemical binder of 40% concentration was applied over the filters after the hydroentanglement process by foam bonding. The filters were dried and cured at a temperature of 170°C in an oven. Nonwoven filters were conditioned under standard testing conditions of 20 ± 2°C and 65 ± 2% R. H. for 24 h before testing. The fineness and length of the polyester fibers used for sample preparation are 3.2 dtex and 60 mm, respectively.

Measurement of filtration parameters

The dust filtration apparatus was used to evaluate filtration parameters, namely filtration efficiency and pressure drop according to ASHRAE standard 52.2.[14] Dust particles in the range of 0.6-180 μm are fed at a constant rate to the filtration device and deposited on the samples having an area of 0.0095 m^2.

Measurement of fiber orientation

The fiber orientation is measured by using image analysis programme "analySIS" version 3.2. The relative frequency of fibers for 10° orientation interval with respect to the crossdirection is computed.[13]

Measurement of pore sizes

The pore sizes were measured on a capillary flow porometer based on the principle of the liquid extrusion porometry technique.[16,17] In this method, a wetting liquid with known surface tension of 15.9 dynes/cm spontaneously fills the pores, and it is then removed by pressurized nonreacting gas (air) to give various types of pore sizes. Three kinds of pores may be present in nonwoven filters, namely closed pores, through pores, and blind pores. Closed pores are not accessible and therefore do not allow passage of liquid and air. The blinds pores terminate inside the material and do not permit the fluid flow. Through pores are open and allow the flow through the medium, and they are important for filtration and drainage applications.[16,17] The important through pore characteristics of a nonwoven filter medium are the smallest pore diameter, the largest pore diameter, and mean pore diameter.[13,16,17]

Cyclic compression

It is performed by the standard cyclic compression testing mode of the porometry instrument.[12] Compression and decompression times used were 23 s and 100 cycles were used for testing. The velocity of traverse of piston for cyclic compression was 4.5 mm/s. Diameter of samples being compressed is

5 mm and applied pressure on the samples is 0.18 MPa.

RESULTS AND DISCUSSION

Condition of conical capillary nozzle and fluid flow simulation

One of the factors for the energy transformation is the condition of the conical capillary nozzle and the nature of the fluid flow through it. It is worthwhile to study this factor for a given water jet pressure. A schematic representation of a typical conical capillary nozzle with length (l); 1 mm, inner diameter (d); 0.12 mm, outer diameter; (D) = 0.3 mm is shown in Figure 1. Generally nozzles are arranged in series in single or double row in a stainless steel jet strip, which runs throughout the width of the machine and placed in different manifolds. A photograph of the jet strip along with nozzles is shown Figure 2. When high-pressure water suddenly enters the nozzle at 90° angle, constricted water jets are formed which are desirable for the hydroentanglement process.[9,10] Constricted water jets are the flow inside the nozzle, which is separated from the nozzle inner wall. These constricted water jets give rise to a condition that allows the downstream air to flow inside the nozzle due to a pressure difference and envelop the water jet.[9,10] So, the flow inside the nozzle is a mixture of two fluids, i.e., water and vapor. A three-dimensional (3D) fluid flow field inside the conical capillary nozzles was simulated by using the re-normalized group (RNG) k–ε model of turbulence along with standard wall functions.[18] Pressure inlet and pressure outlet boundary conditions are used for the simulation purpose. At the wall no slip boundary condition is applied. The mass, momentum, and energy equations are used to solve an unsteady compressible turbulent flow of a mixture of water and vapor inside the nozzle.[18]

A schematic representation of the nozzle coordinate system for simulation purpose is shown in Figure 1. Fluid velocity profiles are calculated at five

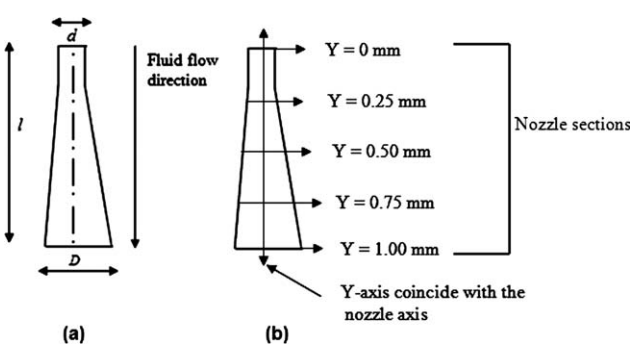

Figure 1 (a) Schematic representation of a conical capillary nozzle and (b) nozzle coordinate system.

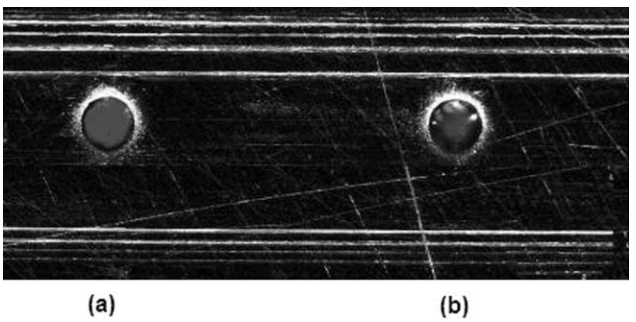

Figure 2 Photograph of the jet strip along with conical capillary nozzles (a) normal nozzle and (b) nozzle with wear.

different normal planes of conical capillary nozzle. Inlet of the nozzle is the place, where fluid first enters, and it is considered as origin. This is the first section, where velocity plots are taken (Y = 0). Then the subsequent sections are taken along the nozzle axis as per the nozzle coordinate system as shown in Figure 1. The fluid flow profiles are simulated and velocities are calculated in these sections.

The CFD results obtained from the water and vapor flow through a normal nozzle and nozzle with wear at 60-bar pressure are shown in Figure 3(a,b). Y = 0 mm indicates the nozzle inlet and Y = 1.00 mm indicate nozzle outlet. Each color in Figure 3 represents a particular velocity value in m/s, red being the highest and blue is the lowest. It can be seen from Figure 3(a) that water is flowing in a straight path with a constant velocity in the middle

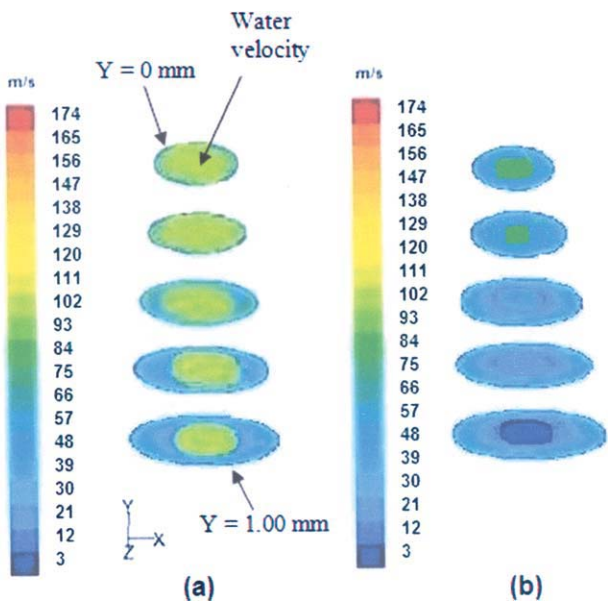

Figure 3 Velocity of water and vapor through a conical capillary nozzle at 60 bar pressure (a) normal nozzle and (b) nozzle with wear. [Color figure can be viewed in the online issue, which is available at www.interscience.wiley.com.]

section of the normal nozzle, whereas the vapors are generated as a result of low-pressure flow around the wall of the normal nozzle at a lower velocity. The average water velocity in the centre of the normal nozzle is around 102 m/s at 60-bar pressure. The corresponding velocity of vapor is around 5 m/s. These vapors may create some kind of recirculation effect in the nozzle. Because their velocity is very less in comparison with the velocity of water, any kind of disturbance to the water flow stream can be neglected.

For effective bonding of the fibers with water jets, it is always desirable to have a constant velocity of flow of water in the centre of the nozzle without any disturbance, so that desired bonding of the fibers can be achieved with the help of impact energy of the water jet. This case is maintained in normal nozzle as shown in Figure 3(a). In the case of a nozzle with wear [Fig. 3(b)], there is significant variation in the velocity of water in the center as a result of irregular flow of fluid at the inlet. Any change in the nozzle condition or wear in the nozzle may be due to the contamination in the supply water or prolonged exposure to a very high pressure. Because of this, the impact of the water jet on the fiber web is uneven and bonding of the fiber will not be uniform. It may result in the unbonded structure or cause of defect on the fabric surface, which are visible in the form of jet streak or jet marks. So, nozzle condition plays an important role in economizing the hydroentanglement process.

Impact energy of the water jets and mechanism of fiber bonding

The perfect utilization of the impact forces of the water jets is related to the velocity of the water jets, and how best this energy is used in bonding the fibers play a major role in energy conservation. If this energy is not properly used, then there is wastage of significant amount of water passing through the permeable surface. So, an additional energy/power is required to force this waste water through the filtration system and then recycling this water for further use. Each time these process is repeated, there will be a significant increase in the water consumption.

The Manifold 2 is the first place, where the entanglement and bonding of the fibers takes place on the exposure side of the fibrous web to the water jets. A series of event takes place during the impact of the water jets at an angle of 90° on the fiber web on the Manifold 2. The water jet maintains its columnar flow until it strikes the fiber web. A schematic representation of the mechanism of fiber bonding and formation of nonwoven fabric is shown in Figure 4. The fiber web is crosslapped (discussed in subsequent section), so majority of the fibers are oriented or arranged in the crossdirection (CD) than in the machine direction (MD). Initially, the fiber web is compressed by the water jet impact, and there is bending of the fibers in the CD and shifting of the position of fibers in the MD. The impact force of a 100 μm diameter of a water jet at an angle of 90° on the fiber web is given by[8]:

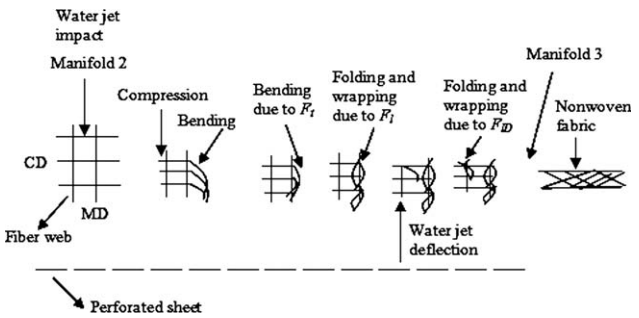

Figure 4 Schematic representations of the mechanism of fiber bonding and formation of nonwoven fabric.

$$F_i = \frac{\pi}{4}\rho v^2 d_j^2 \tag{1}$$

where ρ = density of water (kg/m^3); v = velocity of water jet (m/s); d_j = water jet diameter (m). At 60-bar water jet pressure, the impact force is given by 81.671 mN (ρ = 1000 kg/m^3, v = 102 m/s, d_j = 100 × 10^{-6} m).

When a fiber is subjected to water jet impact, the flow can be split into two mutually perpendicular directions, perpendicular and parallel to the fiber axis. The force acting perpendicular to fiber axis is helpful in further bending and is given by the transverse drag force (F_t). The force acting on parallel to the fiber axis is helpful in folding and wrapping this bent fiber around the adjacent fiber and it is given by the longitudinal drag force (F_l). The above action is predominantly acting on the fibers, which are in the CD. Some of the fibers in the MD are also affected. These drag forces acting on the fiber, which are assumed as smooth circular cylinders, are given by[19,20]:

$$F_t = \frac{1}{2}\rho v^2 S_t C_D \tag{2}$$

$$F_l = \frac{1}{2}\rho v^2 S_l C_D \tag{3}$$

where ρ = density water (kg/m^3); v = velocity of water jet (m/s); S_t and S_l = the projected areas of the fiber on which perpendicular and parallel fluid flow acts (m^2); C_D = drag coefficient (a dimensionless number).

$$C_D \text{ is related to the Reynolds number as : } R_e = \frac{v d_f}{\mu/\rho} \tag{4}$$

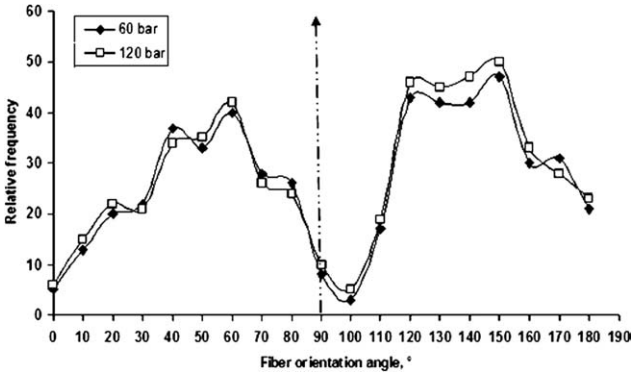

Figure 5 Orientation distributions of fibers in the nonwoven filters.

where d_f = diameter of the fiber (m); μ = viscosity of water (kg/m/s); l = length of the fiber (m). The projected area of a fiber for transverse drag force is given by $S_t = d_f\, l$. The projected area of a fiber for longitudinal drag force is given by $S_l = \pi\, d_f\, l$.

Because fibers are numerous in the web and if there are N number of fibers, the transverse and longitudinal drag forces are given by F_t/N and F_l/N. The values of F_t/N and F_l/N are given by 5.680 mN and 17.837 mN at a water jet pressure of 60 bar (ρ= 1000 kg/m^3, v = 102 m/s, $d_j = 100 \times 10^{-6}$ m, $d_f = 18.2 \times 10^{-6}$ m, $\mu = 1.003 \times 10^{-3}$ kg/m/s, $l = 60 \times 10^{-3}$ m, N = 1000).

Another series of events take place after the above set of actions because of deflection of the water jets from the perforated surface. Energy transfer also depends on the nature of the perforated surface. This surface is such that, it will allow maximum possible deflection of the impacted water jets, so that the other remaining fibers that are not bonded, i.e., the fibers that are in the MD are bonded with this deflected impact force. It was found that 95% of the water jet is deflected back from the perforated sheet and remaining 5% of the water will pass through the perforated sheet and recycled, filtered for using it again. This deflection is possible at 90°, 60°, 45°, or at any other angles. The former deflected angles mainly play important role in bending the fibers in MD and further increasing the frictional contact between the CD fibers by pushing them close to each other. As discussed previously, similar kind of event will take place by the action of drag forces. The MD fibers will be bonded with each other accompanied by increasing the frictional contact of the CD fibers, resulting in a compact structure of the fiber web. This action takes place in Manifold 2 for a particular water jet. Similar type of action is taking place by other water jets, which are on the jet strip. Then the web passes to the Manifold 3, which performs the action on the reverse side of the fabric. The remaining bonding and compaction of the fiber structure is achieved through the Manifold 3, resulting in the formation of the nonwoven fabric. The impact force of the water jets and fluid drag forces play an important role in the mechanism of fiber bonding

Orientation distribution of fibers in the nonwoven filters

A typical orientation distribution of fibers in the nonwoven filters produced at 60 bar and 120 bar, respectively, is shown in Figure 5. The vertical dashed arrow line at 90° angle represents the MD orientation, the CD being perpendicular to this. The lower frequency values in the MD indicate that fewer fibers are oriented in that direction. The higher frequencies values in the other direction indicate the majority of fibers are oriented in the CD, which is due to crosslapping process of laying the web. This type of alignment of fibers generally allows in achieving anisotropic properties.

Pore types, filtration parameters and strength of nonwoven filters

The developed filters were subjected to performance evaluation in terms of changes in pore types, filtration parameters such as filtration efficiency and pressure drop, and breaking strength after cyclic compression. These values are compared with the corresponding values obtained without cyclic compression.

Among the through pores, the smallest and maximum pore diameters are the diameters of the smallest and largest pores, respectively. The mean flow pore (MFP) diameter is related to the filtration efficiency, and it is the diameter of the majority of the pores.[16,17] The pore size of nonwoven filters obtained from porometry before and after cyclic

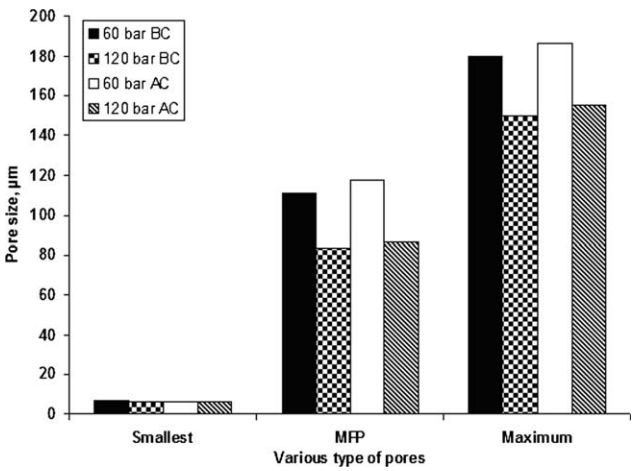

Figure 6 Changes in various types of pore sizes before (BC) and after (AC) cyclic compression.

TABLE I
Filtration Parameters of Nonwoven Filters Before and After Compression

		Filtration parameters			
		Before compression		After compression	
Sample code[a]	Water jet pressure (bar)	Efficiency (%)	Pressure drop (Pa)	Efficiency (%)	Pressure drop (Pa)
S1	60	86.62 (NS)	25.0 (NS)	82.23 (NS)	37.50 (NS)
S2	120	90.40 (NS)	12.5 (NS)	85.41 (NS)	19.0 (NS)

[a] Thickness of S1 : 1.60 mm; S2 : 1.36 mm, before compression. NS: nonsignificance.

compression is shown in Figure 6. First, we discuss the influence of pressure on pore sizes, followed by the influence of cyclic compression on it. With the increase in water jet pressure from 60 to 120 bar, there is a decrease in all the pore sizes for the samples tested before compression (BC). Similar trend is found for the samples produced after cyclic compression (AC). With the increase in water jet pressure, the impact force acting on the fibers increases, which results in the greater entanglement of the fibers. As a result, the neighboring pores are getting covered by the fibers and sizes of various types of pore also reduce. There is a marginal increase in the size of various types of pores after cyclic compression, but this increase is not significant. This may be due to the frictional forces acting at the interfiber contact points are good enough to withstand the cyclic compression. The chances of fiber slippage in such cohesive structures are less that results in not so significant decrease in the pore sizes as evident from Figure 6. Significant test is carried out at 95% confidence interval by using Student *t*-test and this test is also repeated for other performance properties.

The result obtained from filtration test is shown in Table I. With the increase in water jet pressure from 60 to 120 bar, the filtration efficiency increases, whereas the pressure drop decreases for the samples tested before cyclic compression. Similar trend is found for the samples tested after cyclic compression. The increase in filtration efficiency may be due to decrease in MFP diameter, which causes capture and retention of greater amount of dust particles. Coating the filters with the binder helps to reduce the pore size, thereby playing a role in capturing submicron particles. The pressure drop also decreases with the increasing water jets pressure, which is related to the thickness of the samples. A more compact structure with less thickness is produced at high water jet pressure when compared with the more open structure with high thickness is produced with low pressure. The filtration efficiency decreases and the pressure drop increases for samples tested after cyclic compression in comparison to the samples tested before cyclic compression. These changes in filtration properties are not significant.

The strength of nonwoven filters in the MD and CD before and after cyclic compression is shown in Figure 7. With the increase in water jet pressure from 60 to 120 bar, the tensile strength in both the directions increases. The increase in strength in CD is higher in comparison with that in MD for all the cases. This may be due to the preferential fiber alignment in CD direction, which is attributed to the crosslapping techniques used in this study. The increase in strength with the increase in the water jet pressure is due to higher entanglement and consolidation of the fiber structure. There is no significant change in the strength values after compression. The developed air filters show very good performance characteristics for long-term applications with high efficiency and low pressure drop in capturing micron and submicron size particles without any significant changes in strength.

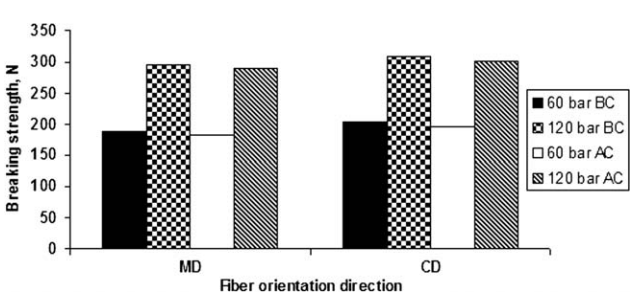

Figure 7 Strength values before and after cyclic compression.

CONCLUSIONS

New high-efficiency filters are developed for air filtration by bonding the nonwoven web with the help of high-pressure water jets. The long-term performance characteristics of the filters are evaluated in terms of changes in pore types, filtration parameters and strength after cyclic compression. The developed filters show very good performance characteristics after prolonged exposure to working condition without any significant changes in above properties.

A mechanism of fiber bonding is proposed on the basis of fluid drag forces and impact force of the water jets.

References

1. Butler, I. The Nonwoven Fabrics Handbook; Association of the Nonwoven Fabrics Industry-INDA: North Carolina, 1999.
2. Patanaik, A.; Anandjiwala, R. D.; Gonsalves, J.; Boguslavsky, L. Paper Presented in Finite Element Modeling of Textiles and Textile Composites Conference; St-Petersburg, Russia, 26–28th September, 2007.
3. Begenir, A.; Tafreshi, H. V.; Pourdeyhimi, B. Text Res J 2004, 74, 178.
4. Berkap, O.; Pourdeyhimi, B.; Seyam, A. Int Nonwoven J 2003, 12, 28.
5. Connolly, T. J.; Parent, L. R. Tappi J 1993, 76, 135.
6. Anand, S. C.; Brunnschweiler, D.; Swarbrick, G.; Russell, S. J. In Handbook of Nonwovens; Russell, S. J., Ed. Woodhead Publishing Ltd.: Cambridge, UK, 2007. pp 201–297.
7. Russell, S. J.; Mao, N. Comp Sci Tech 2006, 66, 80.
8. Anantharamaiah, N.; Tafreshi, H. V.; Pourdeyhimi, B. Exp Fluids 2006, 41, 103.
9. Tafreshi, H. V.; Pourdeyhimi, B. Exp Fluids 2003, 35, 364.
10. Tafreshi, H. V.; Pourdeyhimi, B. Text Res J 2004, 74, 359.
11. Comsol Multiphysics 3.2. User Guide; Comsol AB, Sweden, 2005.
12. Capillary Flow Porometer. Instruction Manual; Porous Materials Inc.: Ithaca, New York, 2005.
13. Image analySIS version 3.2. User Guide, 2002.
14. ANSI/ASHRAE Standard 52.2, 1999.
15. ISO 9073-3, Association of the Nonwoven Fabrics Industry-INDA, Cary, North Carolina, 2005.
16. Jena, A.; Gupta, K. Int Nonwoven J 2003, 12, 45.
17. Mayer, E. Filtr News 2002, 20, 1.
18. Wilcox, D. C. Turbulence Modeling for CFD, 2nd ed.; Dcw Industries: California, 1998.
19. Roberson, J. A.; Crowe, C. T. Engineering Fluid Mechanics, 4th ed.; Fifflin Company: Boston, 1990.
20. Janna, W. Introduction to Fluid Mechanics; PWS Engineering: Boston, 1983.